

EE463 Term Project DC Motor Driver Report

by Drive & Survive

Mustafa Berkay KEBABCI 2575595

Orkun Bera GEDİK 2516185

Sefer İDACI 2575421

Table of Contents

1 - Introduction.....	3
2 - Project Specifications.....	3
3 - Topology Selection.....	3
4 - Component Selection.....	5
5 - Open Loop Simulation.....	6
6 - Controller Implementation.....	11
7 - Thermal Simulation.....	18
8 - PCB and Case Design.....	20
9 - Targeted Bonuses.....	25
10 - Conclusion.....	25

1 - Introduction

This project focuses on designing and simulating a high-performance DC motor drive system. The chosen topology combines a three-phase diode rectifier with a buck converter. The rectifier converts three-phase AC input into DC, while the buck converter ensures voltage regulation to meet motor specifications. This hybrid approach balances simplicity, cost-effectiveness, and operational efficiency, making it suitable for industrial-scale applications. Through this project, we aim to explore key aspects of power electronics design, including component selection, thermal considerations, and control strategies, culminating in an open-loop simulation to validate performance.

2 - Project Specifications

The design specifications for the DC motor drive system are as follows:

Input: Three-phase AC voltage (RMS) from the variac up to 105 V line to line RMS.

Output: Regulated DC voltage up to 240 V.

Power Rating: 2 kW with provisions for additional load tolerance.

Motor Specifications:

Armature resistance: $0.8\ \Omega$

Armature inductance: 12.5 mH

Rated current: 11 A (steady-state)

Rated voltage: 220 V

Efficiency Goal: Greater than 85% at full load.

Topology Requirements:

Rectifier: Low ripple and high conversion efficiency.

Buck Converter: Efficient step-down operation with minimal losses.

Thermal Constraints: Ensure safe operating temperatures using heatsinks and fans.

Control Strategy: Open-loop control for initial validation, with provisions for closed-loop feedback in future enhancements.

3 - Topology Selection

There were 3 basic topologies that we thought as reasonable:

- 3 Phase Thyristor Rectifier
- Single Phase Diode Rectifier + Buck Converter
- 3 Phase Diode Rectifier + Buck Converter

3 Phase Thyristor Rectifier

The 3-phase thyristor rectifier is a robust solution for converting AC to DC with dynamic voltage control capabilities. In this topology, thyristors are used to regulate the rectification process by adjusting their firing angles, allowing precise control over the DC output voltage directly from the AC input. This eliminates the need for additional DC-DC conversion stages, such as a buck converter, in applications requiring adjustable voltage levels.

The primary advantage of this approach is the ability to dynamically control the output voltage to match varying load requirements. This makes the topology highly suitable for industrial drives, variable-speed motor controls, and applications demanding high power levels. By simply modifying the firing angle of the thyristors, the system can adapt to different operational conditions without requiring complex additional circuitry.

Despite its benefits, the thyristor rectifier has some drawbacks. The firing circuitry adds complexity to the system, and the introduction of harmonic distortion into the AC supply requires the use of filters to comply with power quality standards. These filters can increase both the cost and the size of the overall system. Nevertheless, the thyristor rectifier remains a reliable and efficient choice for high-power applications, offering the flexibility to adjust voltage levels directly at the rectification stage.

Single Phase Diode Rectifier + Buck Converter

This is a simpler and more cost-effective solution. The single-phase diode rectifier converts AC to a fixed DC voltage, which the buck converter subsequently regulates. This topology is widely used in low to medium power applications, such as small power supplies or household appliances. Its simplicity and low cost make it appealing for less demanding applications. However, the single-phase design inherently results in higher ripple in the rectified DC output, which increases the demand on the buck converter's filtering stage. Furthermore, its power-handling capability is limited compared to three-phase systems, making it unsuitable for high-power industrial applications.

3 Phase Diode Rectifier + Buck Converter

This topology combines the benefits of three-phase rectification with the simplicity of diode-based rectifiers. The three-phase diode rectifier provides a relatively smooth DC output with lower ripple compared to single-phase rectification, thanks to the three-phase input. This minimizes the filtering requirements and enhances the efficiency of the buck converter stage. The absence of thyristors simplifies the circuit, reducing both cost and maintenance. This topology is particularly well-suited for high-power applications where

Chosen Topology: Three-Phase Rectifier with Buck Converter

The combination of a three-phase diode rectifier and a buck converter was selected to fulfill the design objectives. This topology offers:

- **Advantages:**
 - High efficiency due to reduced conduction losses in the rectifier.
 - Low ripple in the rectified output compared to single-phase rectifiers.
 - Simplicity in control and implementation.
 - Cost-effectiveness, as the topology uses fewer components compared to thyristor-based systems.
- **Rectifier:** The three-phase diode rectifier converts the AC input into DC with minimal ripple. The output voltage is approximately 1.35 times the RMS line-to-line voltage.
- **Buck Converter:** This stage regulates the rectifier's output voltage to meet the motor's requirements. The converter operates using an IGBT or MOSFET for switching and a freewheeling diode for continuity during off periods. A duty cycle control mechanism adjusts the output voltage.

4 - Component Selection

Rectifier Components

- **Capacitors:** The rectifier output is filtered using:
 - $3 \times 470 \mu\text{F}$ electrolytic capacitors
 - $1 \times 100 \mu\text{F}$ electrolytic capacitor
 - $3 \times 10 \text{ nF}$ ceramic capacitorsThese components work together to reduce ripple and meet the design criteria of 1% voltage ripple.
- **Rectifier Module:** 36MT160 (1600 V, 47.5 A) three-phase bridge module for efficient and compact AC-DC conversion.

Buck Converter Components

- **Switching Device:**
 - IGBT or MOSFET: IXGH24N60C4D1 or equivalent with:
 - Voltage rating: 600 V
 - Current rating: 24 A
 - Low $R_{ds(on)}$ for reduced conduction losses.
- **Freewheeling Diode:**
 - High-speed diodes (e.g., DSEI30-06A) capable of withstanding the peak inverse voltage and current ratings.
 - Reverse Voltage (ΔV_{RRM}): 600 V
 - Average Forward Current (ΔI_F): 30 A
- **Freewheeling Diode:**
 - DSEI30-06A for fast recovery and low switching losses.

Control Circuitry

- **Gate Driver:** TLP250 optocoupler for isolation and gate signal amplification.

- **Microcontroller:** Arduino Nano for generating PWM signals with adjustable duty cycles.
- **Current Sensor:** Allegro Microsystems ACS712 (30 A rating) for monitoring and protection.
- **Arduino Infrared Receiver Sensor:** Capable of detecting obstacles within 2–30 cm with a 35° detection angle. It outputs a low-level signal when an obstacle is detected and allows adjustable detection distance via a potentiometer. It operates at 3.3–5V and interfaces directly with microcontroller I/O ports for integration.

5 - Open Loop Simulation

The open-loop simulation focuses on analyzing the performance of the rectifier and buck converter under full load conditions. This analysis highlights the system's ability to supply the necessary torque and speed to the DC motor while maintaining voltage stability and minimizing ripple.

The input AC voltage is $104 \times \sqrt{2}$ (approximately 147 V peak), which is rectified by the three-phase diode rectifier to produce 240 V DC with a ripple of less than 1%. The rectified output is then regulated by the buck converter operating at a switching frequency of 5 kHz. This frequency ensures efficient conversion and ripple minimization in the DC output.

To achieve the rated speed of 1500 RPM under a 2 kW load, a duty cycle of 0.93 is used. At this operating point, the motor produces a torque of approximately:

$$T = P / \omega = 2000 / 157 \approx 12.75$$

where ω is the angular velocity in rad/s, corresponding to 1500 RPM.

Key waveforms were observed during the simulation:

Rectifier Output Voltage: The rectified DC voltage showed minimal ripple, confirming the effectiveness of the capacitor network in filtering the output.

Buck Converter Output Voltage: At a duty cycle of 0.93, the buck converter provided a stable voltage to meet the motor's operating requirements.

The simulation demonstrates that the system operates efficiently under worst-case load conditions, supplying the required voltage and torque. The minimal ripple in the output voltage enhances the motor's operational stability and reduces stress on the system components. This performance validates the suitability of the selected topology for industrial motor drive applications. The basic topology schematic can be observed in Figure 5.1.

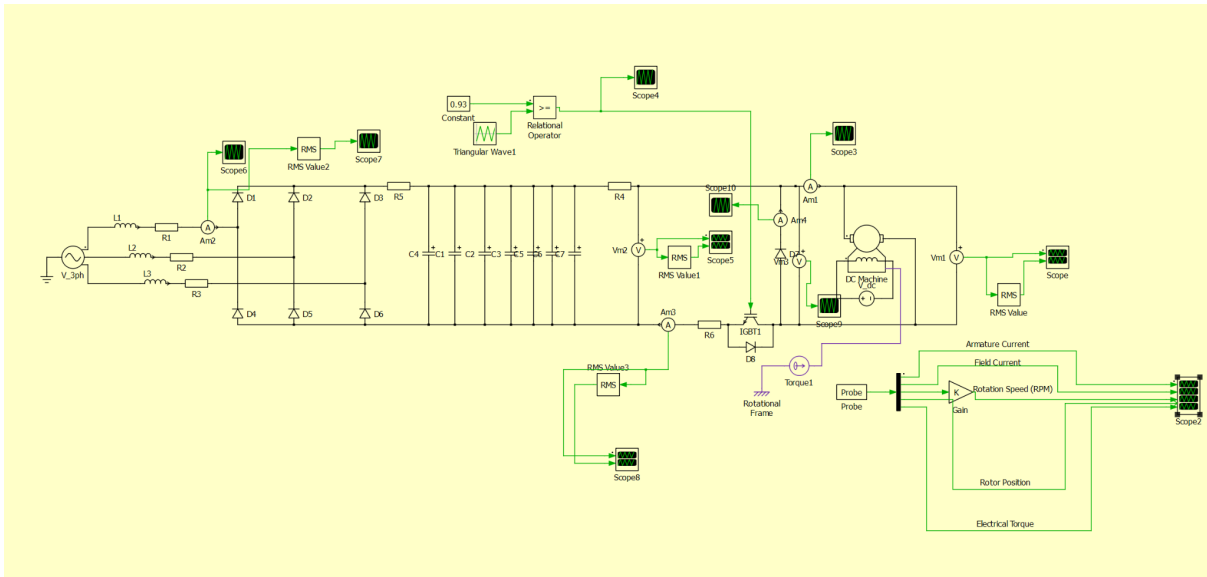


Figure 5.1: Open Loop Simulation Schematic

As we can observe in the Figure 5.2 the input line current THD is about 50.75% which is a large value but feasible for our operation and as we can observe the current is in the limit of our 3-Phase rectifier rated current since it is not commercially viable product for now it is okay but if we were to convert this project to a product we should reduce it to about 5% according to IEEE regulation.

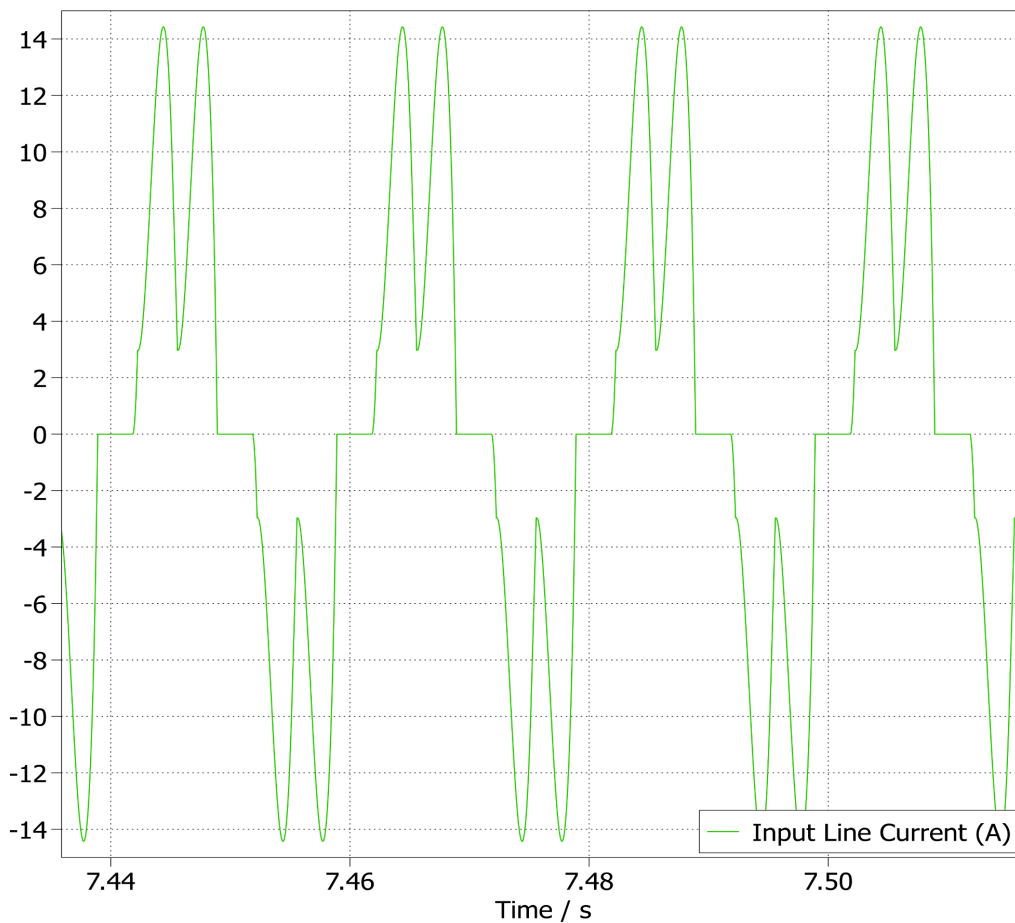


Figure 5.2: Input Line Current vs. Time(s) Graph

As we can observe in Figure 5.3, the rectifier output voltage showed minimal ripple less than 1%, confirming the effectiveness of the capacitor network in filtering the output. Also we can observe that the input voltage is in the rated voltage range of our 3-Phase rectifier and thus we again observed that it is an appropriate product for both voltage and current requirements.

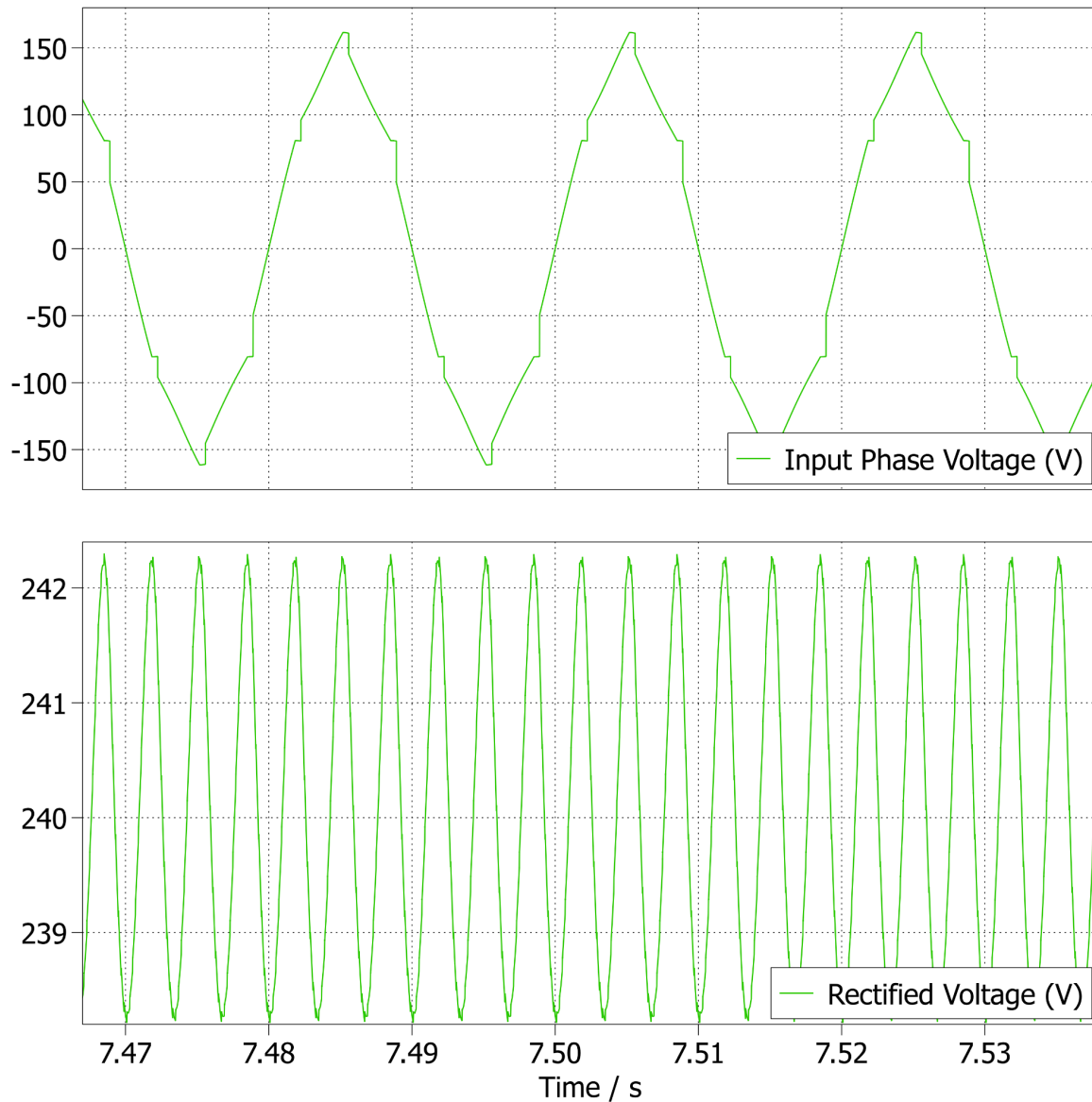


Figure 5.3: Input Phase Voltage and Rectifier Output Voltage vs. Time(s) Graph

As we can observe in Figure 5.4, both the IGBT Current and IGBT VCE we can observe that our IGBT selection was appropriate with enough headroom. This headroom will be an important asset for controller design and potential real life discrepancies.

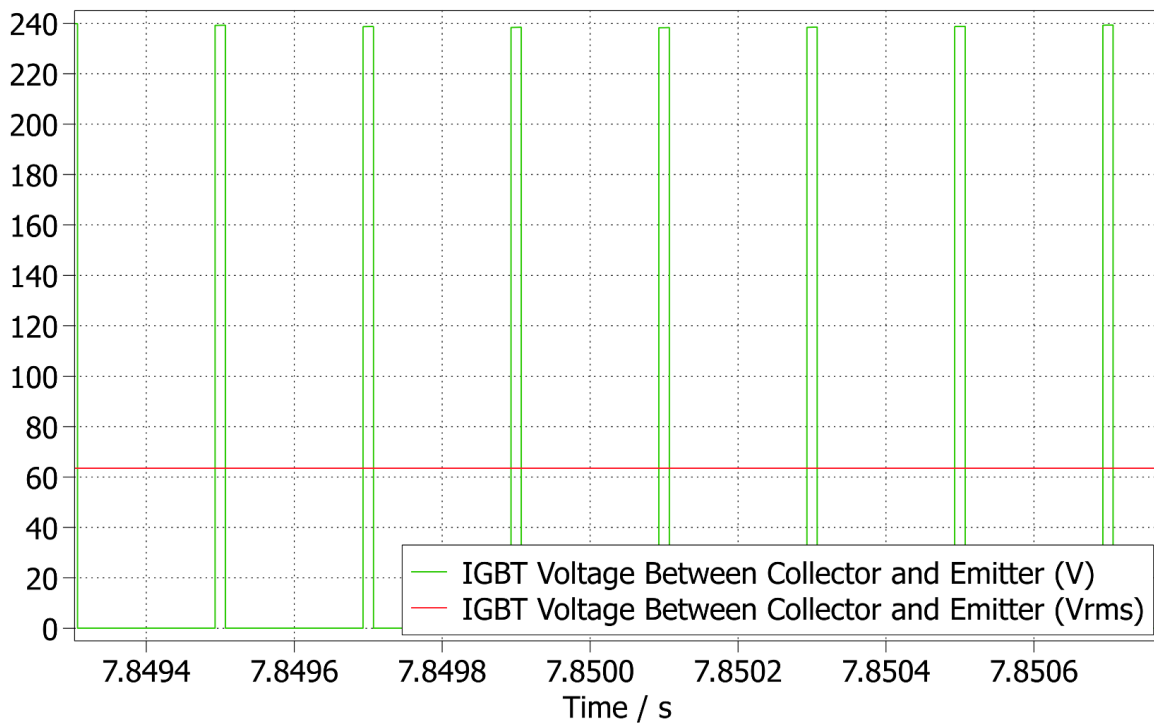
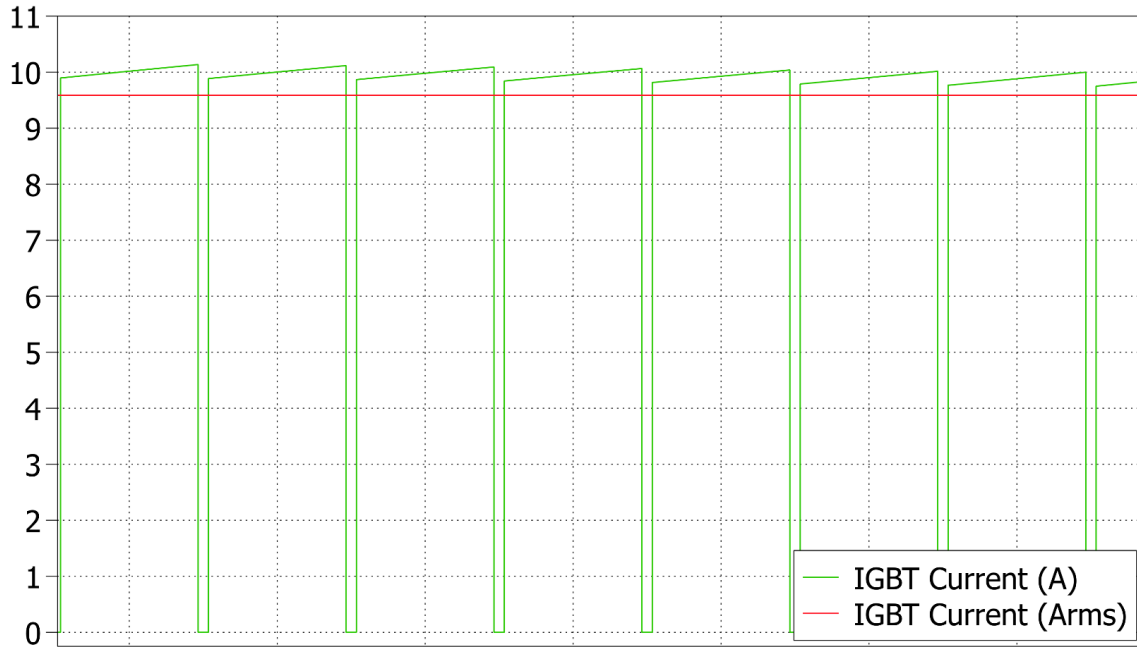


Figure 5.4: IGBT Collector Current and IGBT V_{CE} Voltage vs. Time(s) Graph

As we can observe Figure 5.5, Max Output Voltage is about 240 V and with duty cycle of 0.93 we are achieving the rated voltage of 220 V for 1500 RPM operation without field-weakening. For the command of Max Output Voltage of 180 V we can achieve the total speed of:

$$\omega = 1500 * 180/220 = 1230 \text{ RPM}$$

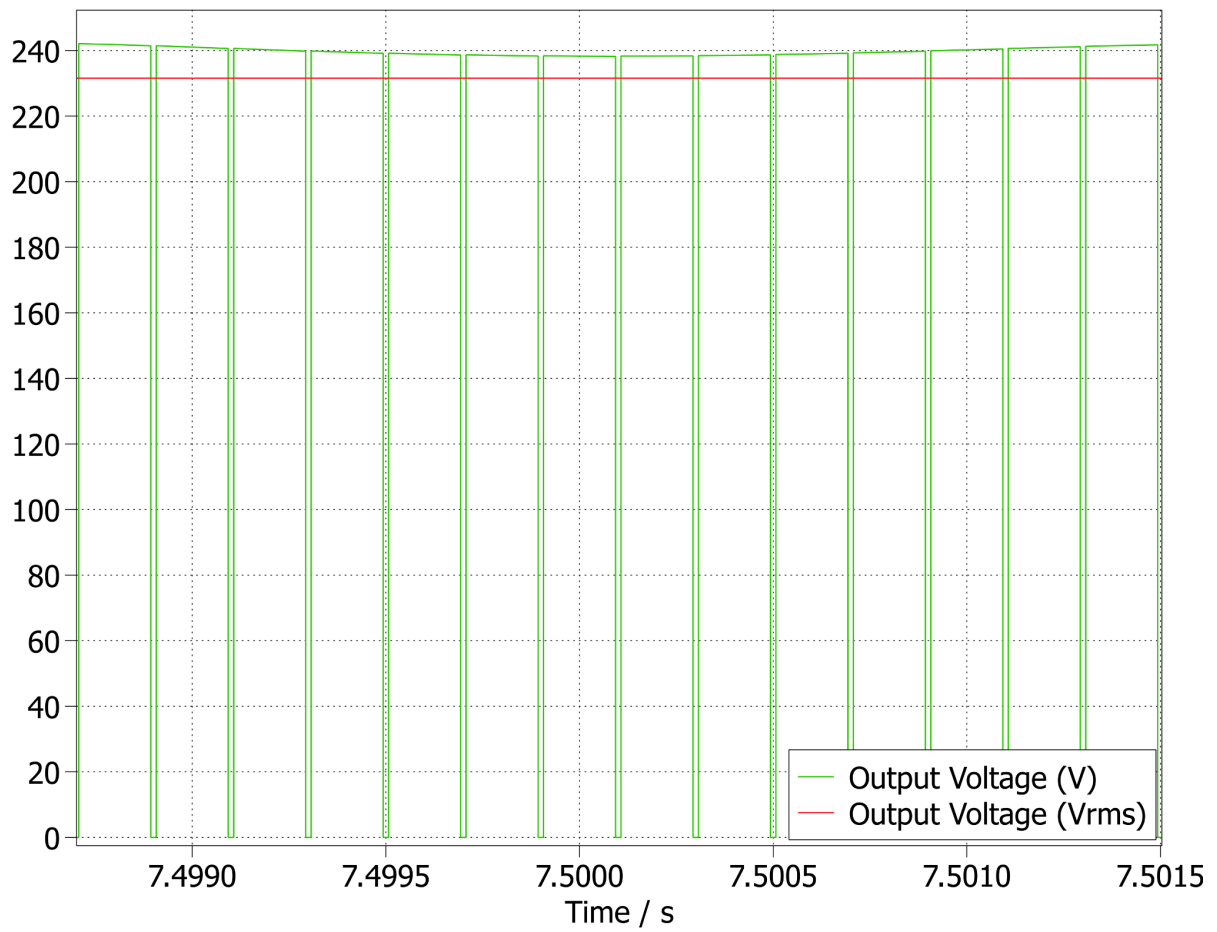


Figure 5.5: Output Voltage vs. Time(s) Graph

As we can observe Figure 5.6, the motor's internal parameters are in steady state. We can observe that our topology is working as expected for an output of 2 kW enough for a kettle to boil water. We can observe the 1500 RPM with duty cycle of 0.93 for a 2 kW output.

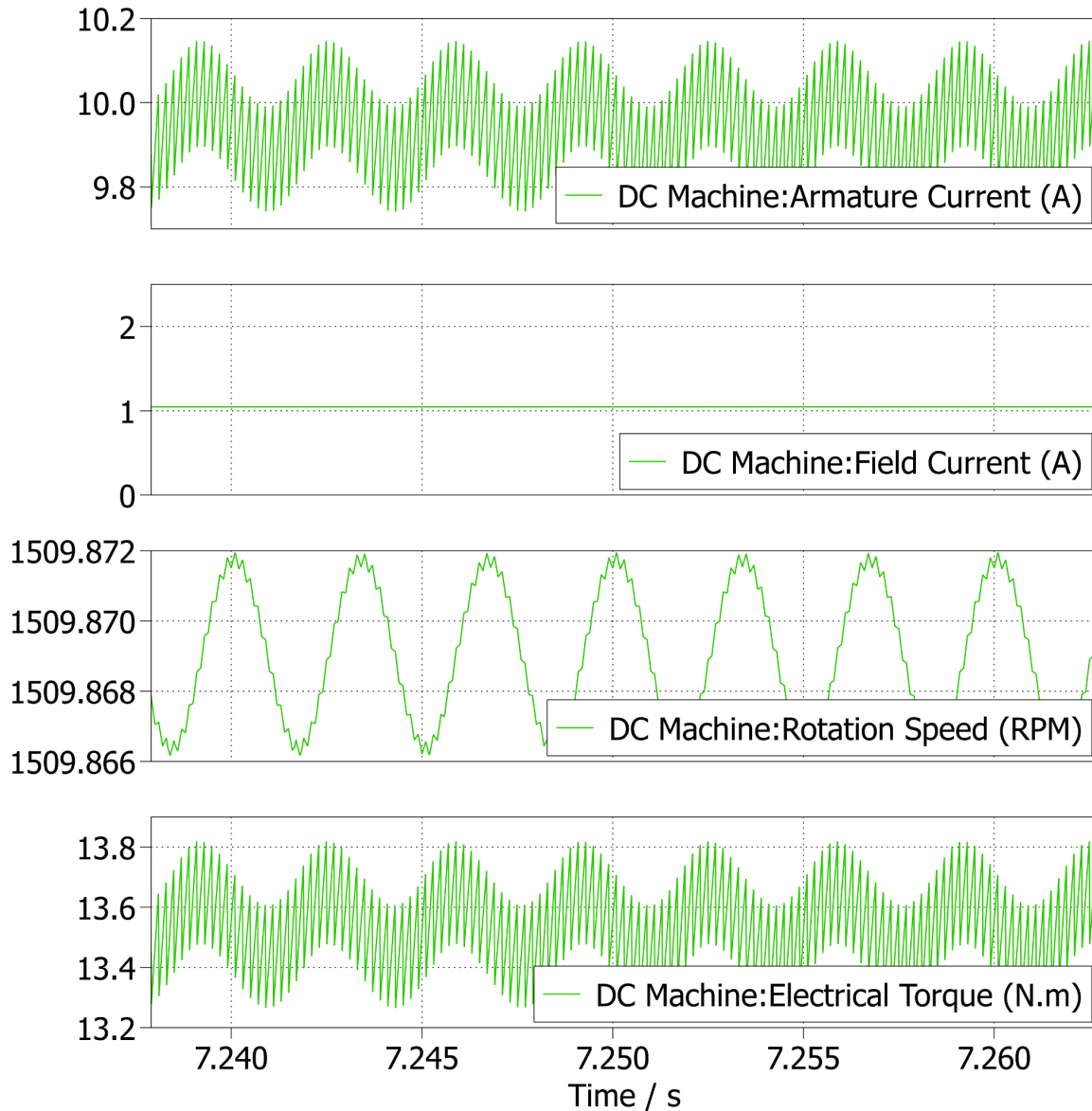


Figure 5.6: Motor Output Parameters

6 - Controller Implementation

The open loop DC Motor + Rectifier system is a stable system. In this project we are tasked to control the speed of the DC machine without allowing high inrush currents to the system. Figures 6.1 and 6.2 show responses of the open loop system on PLECS and Simulink simulation environments. On both plots it is clear that a high inrush current is present, most probably causing EMI problems and it probably damages electronics or the DC motor itself. Secondly it can be seen that even though the setpoint for the DC motor is given as Responses of both applications are very similar hence it is applicable to use Simulink for controller tuning. All components on all Simulink simulations are assumed to be ideal and the non-idealities are added to the components on PLECS simulations. Throughout this section controller tuning and implementation steps are made on Simulink and will be explained with Simulink graphs. At the end, the controller will be put on a final simulation on PLECS with thermal models etc. and the results will be explained furthermore.

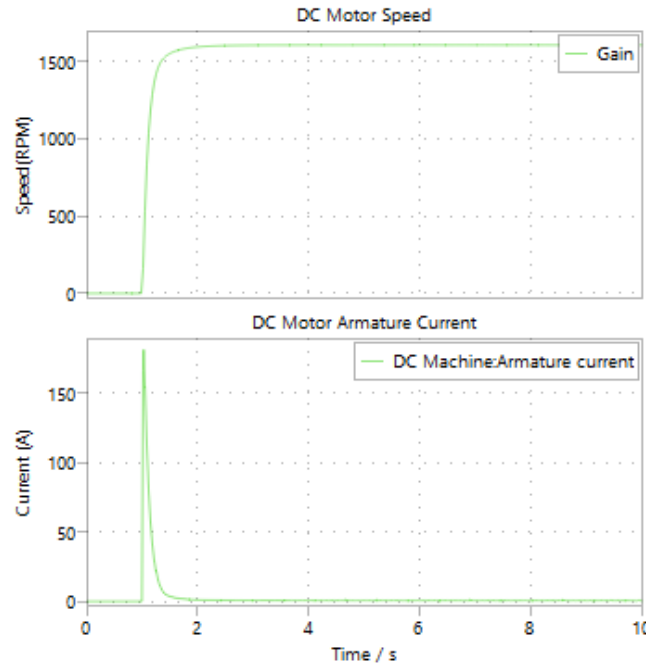


Figure 6.1: Open Loop Step Response of the DC Motor on PLECS.

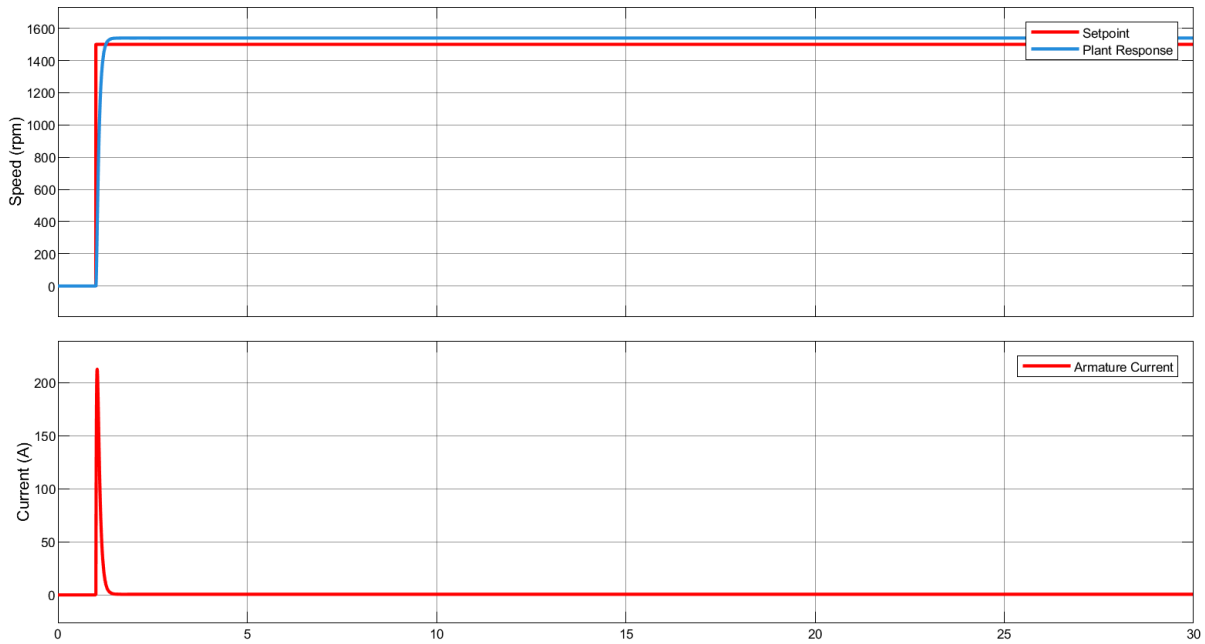


Figure 6.2: Open Loop Step Response of the DC Motor on Simulink.

On the figure it can be observed that the system has a 50ms time constant. It is a rapid time constant considering the rise in the armature current during the process. In order to design a controller for this system, the overall process should be linearized accordingly. IGBT's and diodes are in general nonlinear elements and they should be avoided during linearization processes. Assuming a fixed rectified voltage (240V) and linearizing the Buck converter as DV_{in} , the block diagram on Figure 6.3 can be obtained. Note that the actual simulation on which the tuning processes are made is different from this figure but the working principles of the linearized simulation is same as the system presented on Figure 6.3

Throughout the controller designing process, speed and current measurement transfer functions are assumed to be unity for sake of simplicity. The speed measurements will be made by the infrared sensor which will try to detect white ethicets turning around the motor shaft. For a specified amount of time the microcontroller will count the amount of white object crossings and calculate the RPM value of the motor accordingly. The current measurements will be made by the ACS712 analog current measurement IC device which will generate an analog voltage depending on the current flowing through the armature. In reality transfer functions regarding these processes should also be considered but in order to obtain the transfer functions of these devices, they should be implemented physically and necessary system identification processes should be employed.

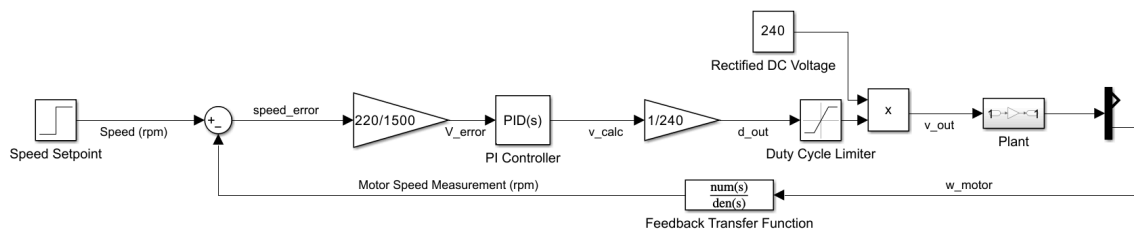


Figure 6.3: Linearized Plant Model Block Diagram.

A PI controller is implemented to slow down the plant time constant to 5s. Step response of the plant with the PI controller can be observed on Figure 6.4. Inspecting the figure, it can be observed that the physical system speeds up gradually and it follows the speed reference given to the controller. Observing the armature current on the DC machine, at startup it makes an impulse of 11 amps. The open loop system also makes an impulse of 150-200 Amps on the armature current but on the closed loop controller this peak is reduced to almost 1/10 on the original value.

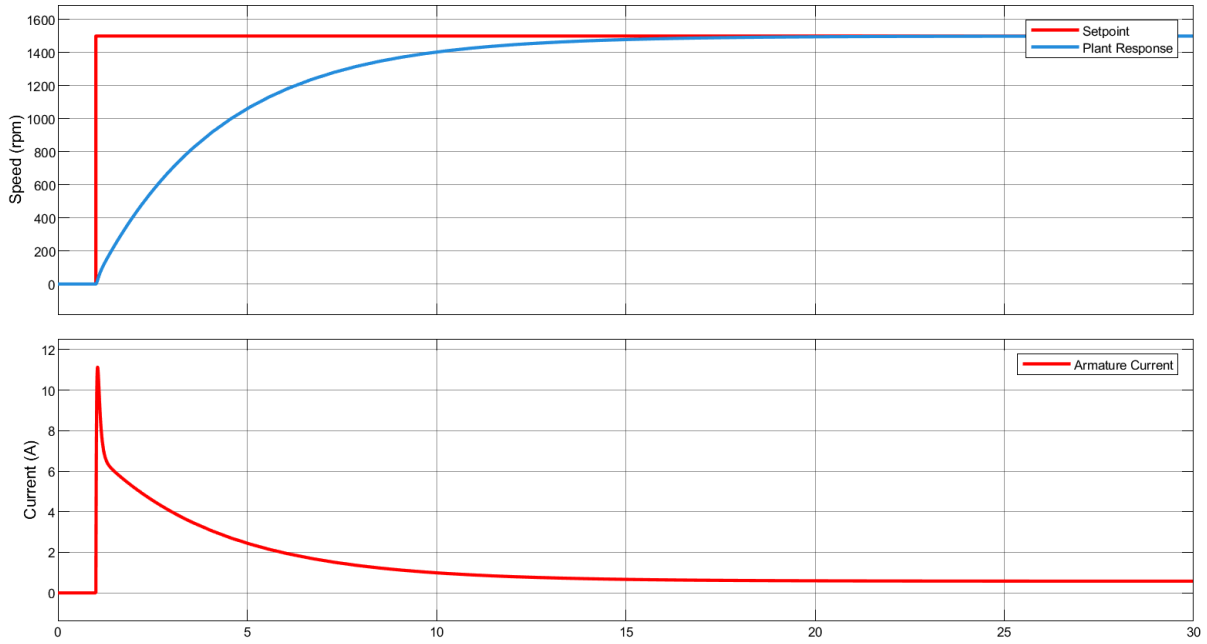


Figure 6.4: Closed Loop Step Response of the PI Controlled DC Motor on Simulink.

Considering the maximum current ratings, this controller can be used on the DC motor; however, just after the starting time of the response, a current with a high rate of increase (500A/s) is present on the armature. This rapid increase in the current can cause problems on the components and the motor itself. In order to overcome this problem, the derivative of the armature current will be considered by the control process somehow. Secondly, there will be high frequency noise on the armature current induced by rapid switching of semiconductor devices, so a filtered derivative should be implemented instead. Additionally we do not want the controller to respond to steady value of the current (if the motor is operated under significant load, there will be significant current which we do not want our controller to respond to) hence the derivative of the current should be given as a disturbance to the system. Figure 6.5 includes the modified block diagram for this structure.

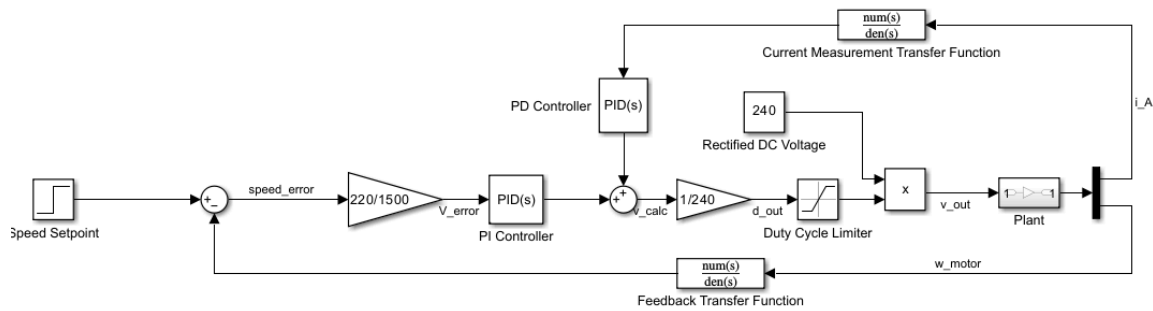


Figure 6.5: Modified Linearized Plant Model Block Diagram.

Transfer function of the general filtered derivative can be written as follows:

$$G(s) = D \frac{N}{1 + N \frac{1}{s}}$$

Bode plot of this transfer function with $D = 2$ and $N = 6$ can be inspected under Figure X.x+5. Step response of the overall system with the filtered derivative presented at Figure X.x+5 can be analyzed on Figure 6.6.

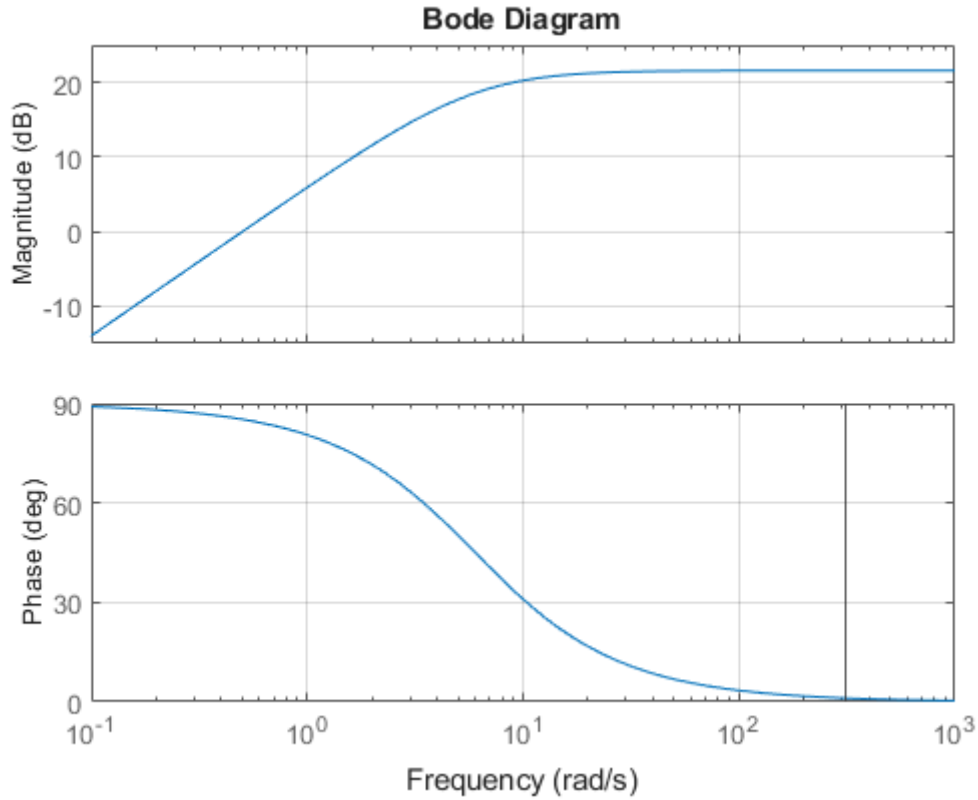


Figure 6.6: Frequency Response of the Implemented Filtered Derivative.

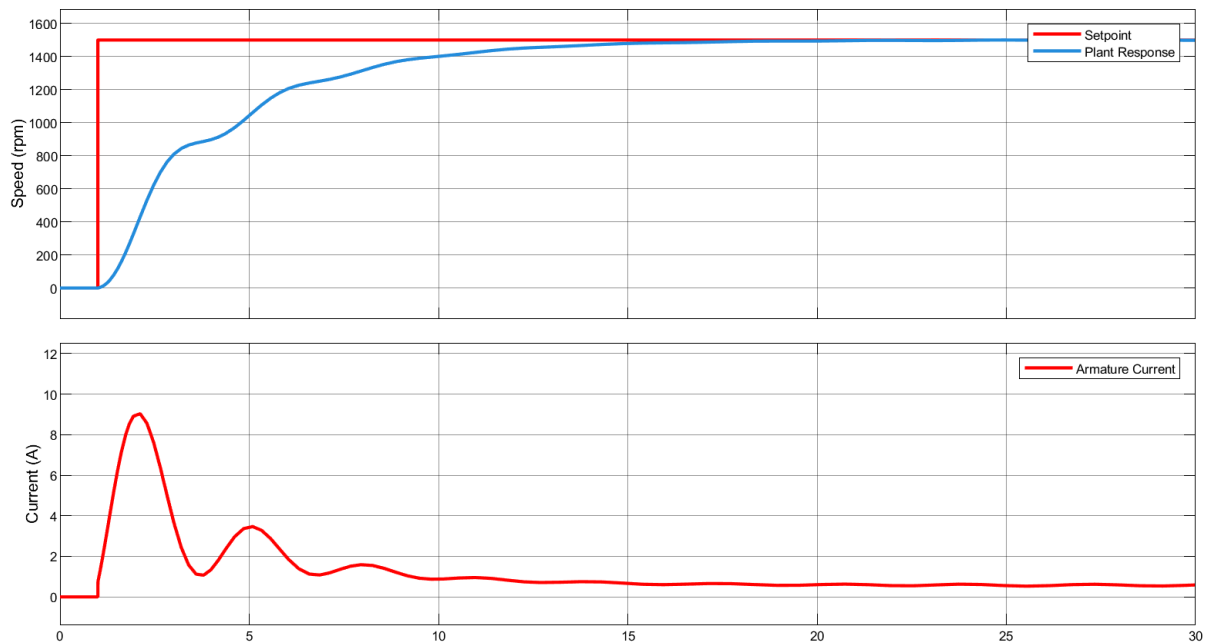


Figure 6.7: Closed Loop Step Response of the Modified PI Controlled DC Motor on Simulink

On Figure 6.7 maximum rate of change of the current (at the beginning of the response) is measured as 12.86 A/s. Settling time of the unmodified and modified PI controllers are almost the same. Another thing that should be noted is the tiny oscillations at the speed of the plant. This behavior is a side result and in general unwanted however considering the improvements on current, it is an acceptable side effect.

After concluding the controller design process, it is tested on the real circuit with ideal elements. Rectifiers, capacitors, inductors, IGBT's are all assumed to be ideal and step response of the overall system can be observed on Figure 6.8. Observing the figure, settling time of the plant remains unchanged even with the presence of high frequency components at the armature current. The controller is also tested on the “tea bonus” scenario, As calculated in Open Loop Simulation section, at 1500 rpm, the tea kettle behaves as a mechanical load with 12.75 N.m torque. As the motor speed increases, the torque that the kettle applies is assumed to increase linearly. On Figure 6.9 the scenario is simulated on the linearised system and on Figure 6.10 it is tested with ideal converter circuits. The controller does not respond to the steady state value of the current but it acts on the transient.

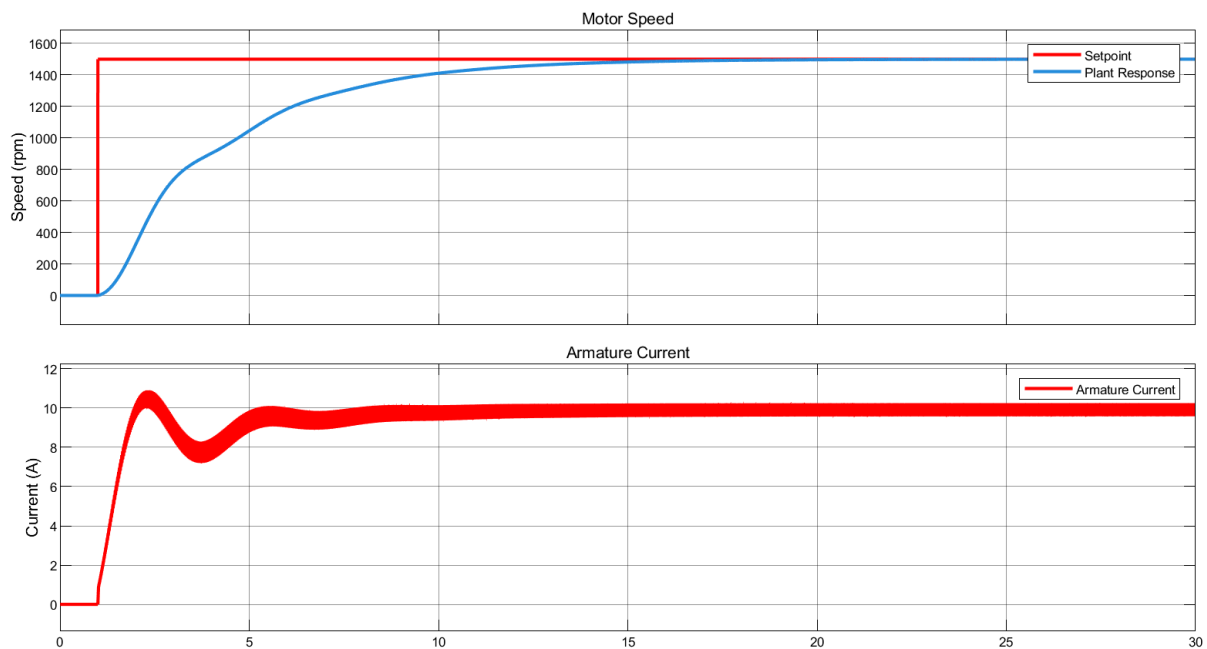


Figure 6.8: Step Response of Overall Closed Loop System on Ideal Converter Circuits.

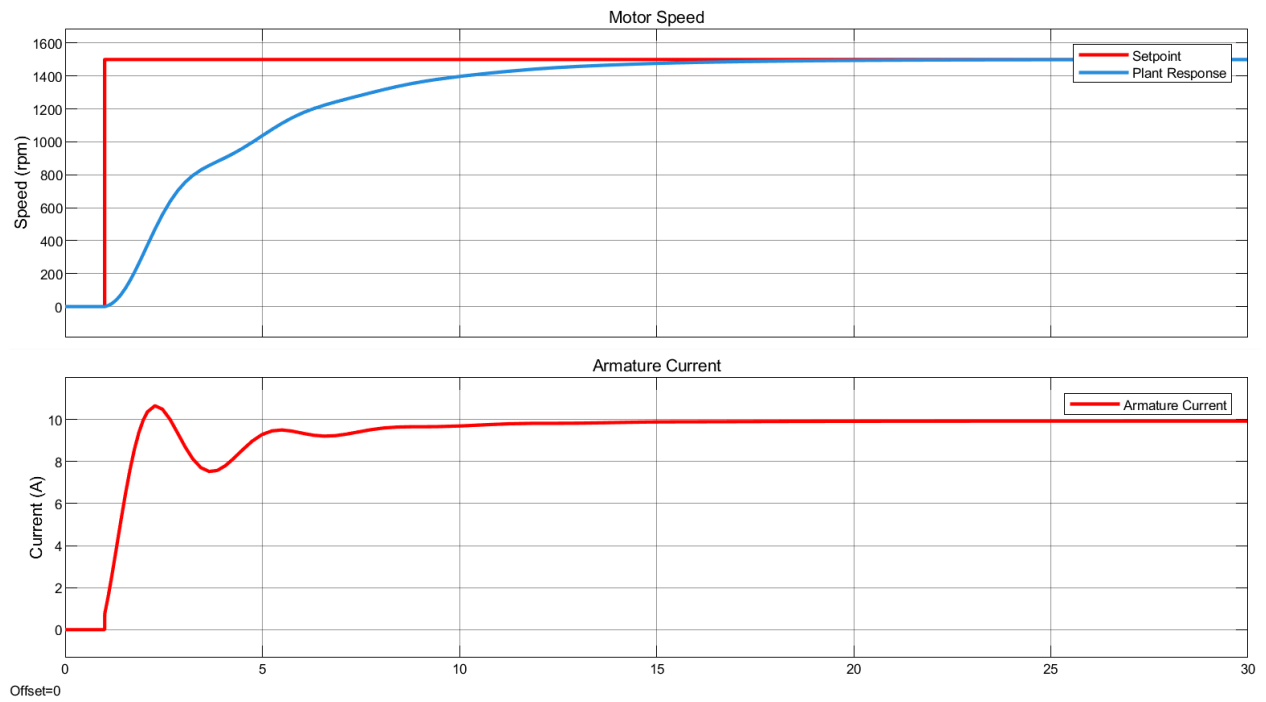


Figure 6.9: Step Response of Overall Closed Loop System on Linearised Tea Bonus System.

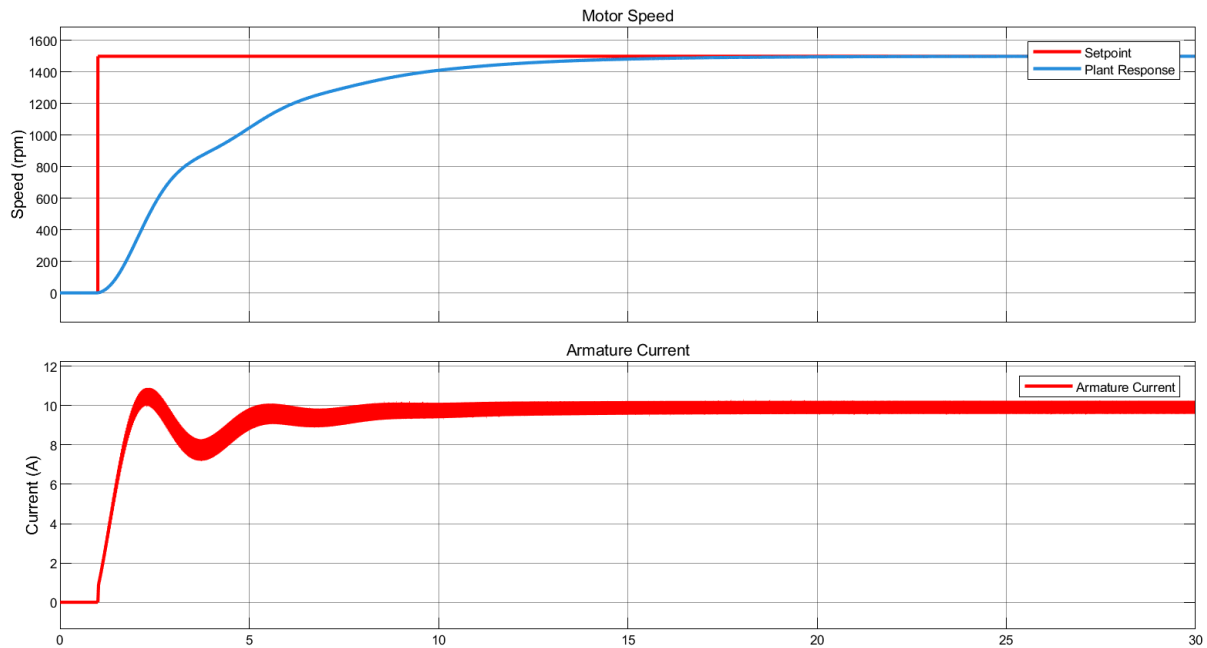


Figure 6.10: Step Response of Overall Closed Loop System on Tea Bonus System with Ideal Converters.

With the selection and modelling of power electronic components with thermal models, the overall control system is tested on the PLECS environment. On Figure 6.11 results can be inspected. Detailed circuit schematic can be inspected at Figure 7.1 on the Thermal Simulation section. As anticipated, the controller works as intended ignoring higher current ripples. Even with the presence of them, the machine reaches the rated speed within a reasonable time.

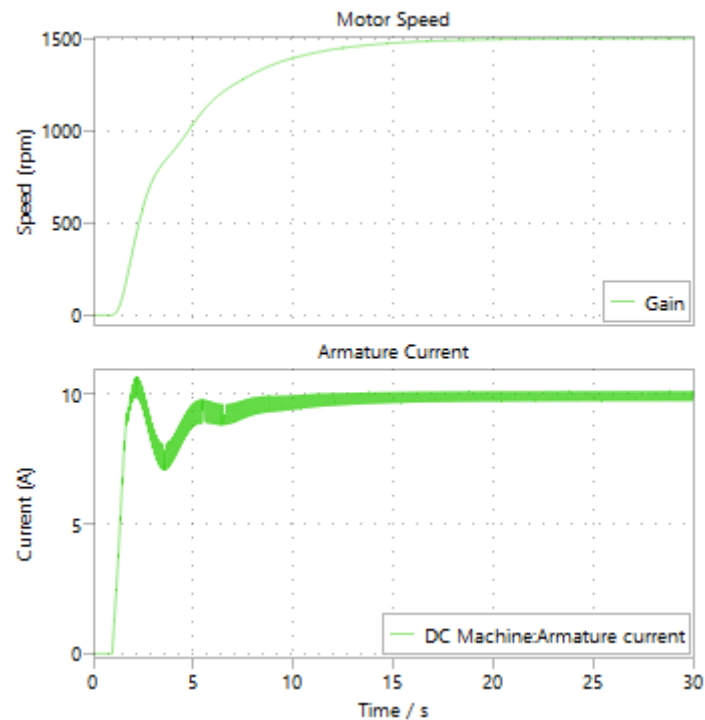


Figure 6.11: Speed and Current Measurements of the DC Motor on Final Simulation.

7 - Thermal Simulation

Power electronics components are designed to operate under several temperature limits. It is important to have thermal knowledge on these devices and operate the system accordingly. In this project three components are the most temperature sensitive devices: the three phase rectifier, IGBT and the freewheeling diode. In this section, thermal PLECS models of these devices are prepared according to the information provided by the manufacturer. Later, depending on the thermal model and losses, temperature difference between junction and cases of the components are calculated and applicable cooling devices are selected. It should be noted that depending on the load and duty cycle, average current passing through the components and the amount of average current flowing through IGBT and diode changes hence for different load and speed scenarios some components heat up more. For the final thermal design, heatsink thermal resistances are chosen for the worst case of each component.

On Figure 7.1 the overall simulation schematic with both thermal models, closed loop controller and power electronic device models present. In Table 7.1, thermal resistance values of the components are summarized. On Table 7.2 thermal information about these devices are provided. In this table specified numbers are taken from steady state operation when the device temperatures, losses reach to a steady state.

Even though there is a “chosen heatsink” option on Table 7.1 the PCB is inserted into a box with heatsinks coming out from three sides. Specified heatsink values are maximum values associated with the components and are chosen from commercial heatsinks. The designed box will certainly provide thermal resistance values smaller than the chosen heatsink options.

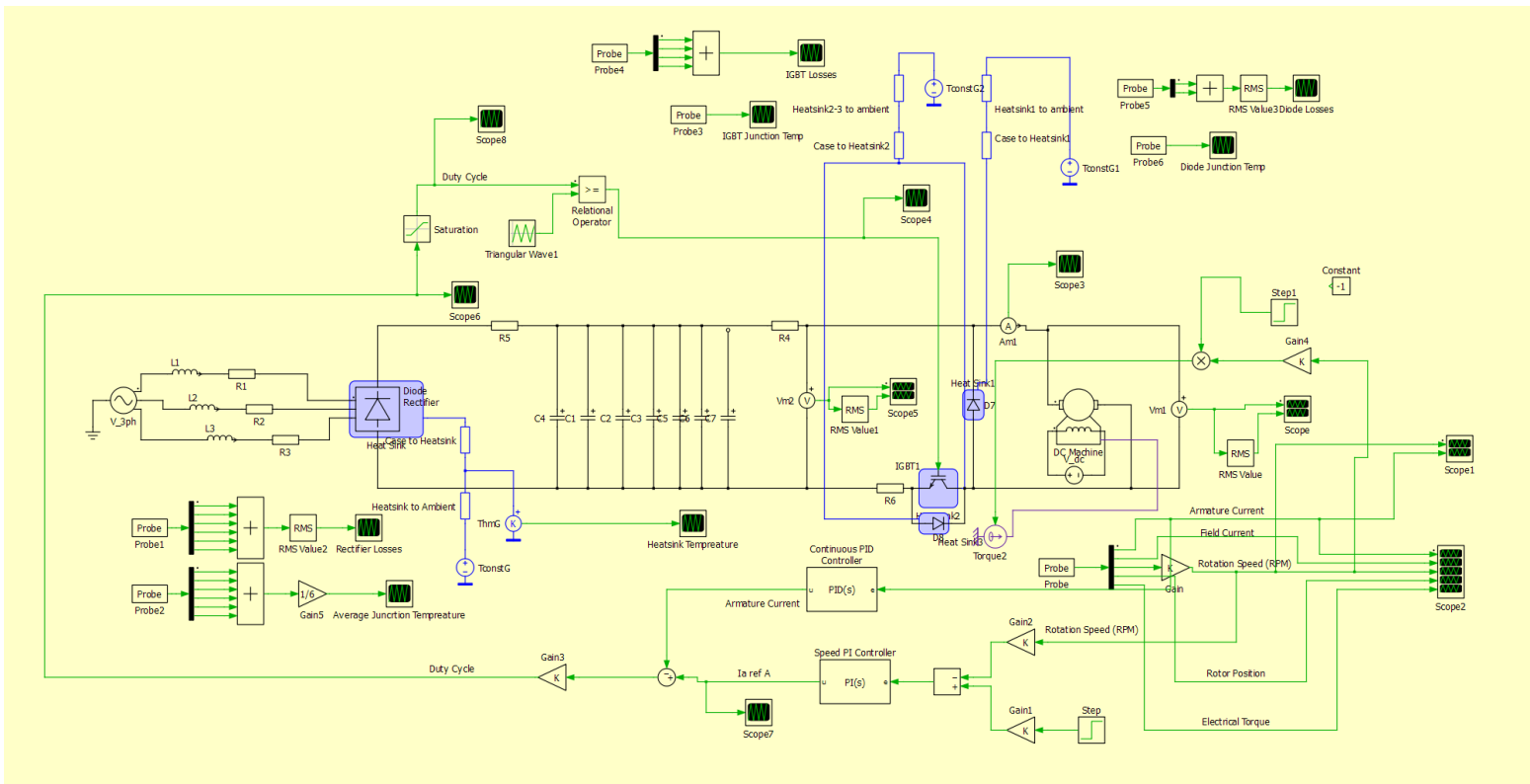


Figure 7.1: The Most Detailed Simulation of the Overall System.

Table 7.1: Thermal Parameters of the Components

Component Name	Maximum Allowed Junction Temperature (C)	Steady State Junction to Case Resistance (K/W)	Steady State Case to Ambient Resistance (K/W)	Chosen Heatsink Resistance (K/W)
36MT160	120*	1.35	0.2	3.32
IXGH24N60C4 D1	150	0.65	0.21	5.25
IXGH24N60C4 D1 Body Diode	150	1.6	0.21	5.25

cables was determined based on the current passing through them. Nine holes were allocated for cables, three were designated for AC input, two for motor connections, one for a 12V external source, and the remaining three for jumper connections to interface with the IR sensor board. The top and bottom views of the board are shown below.

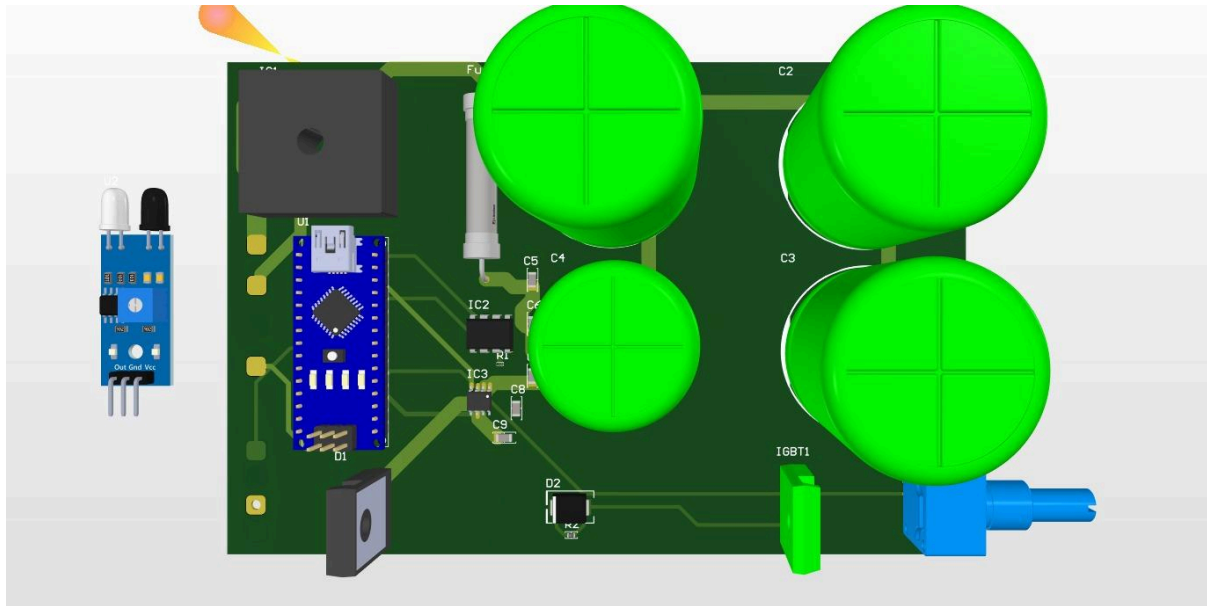


Figure 8.2: Top View of the Board

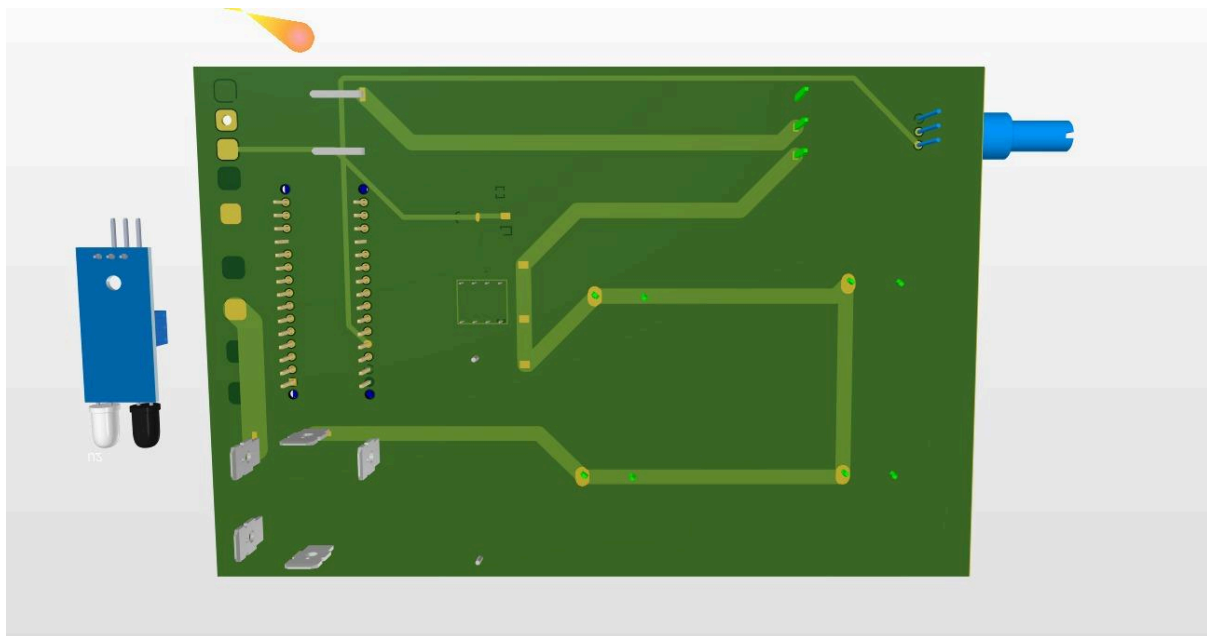


Figure 8.3: Bottom View of the Board

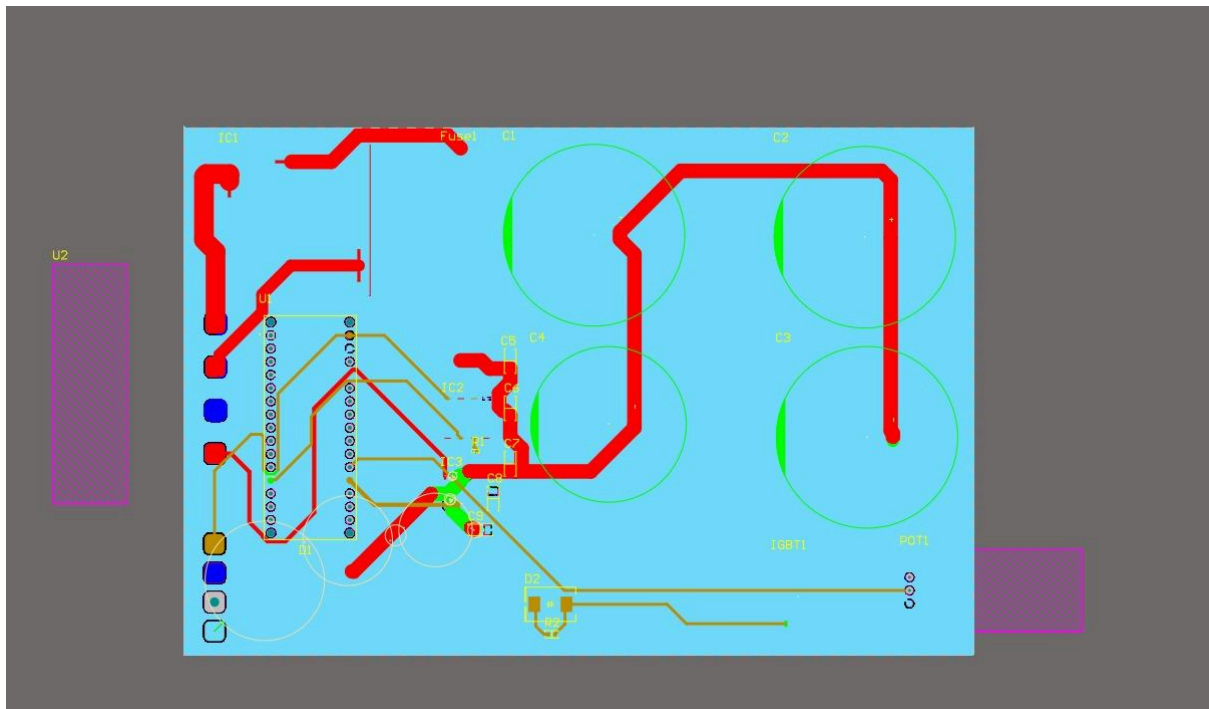


Figure 8.4: Copper Paths of Top Layer

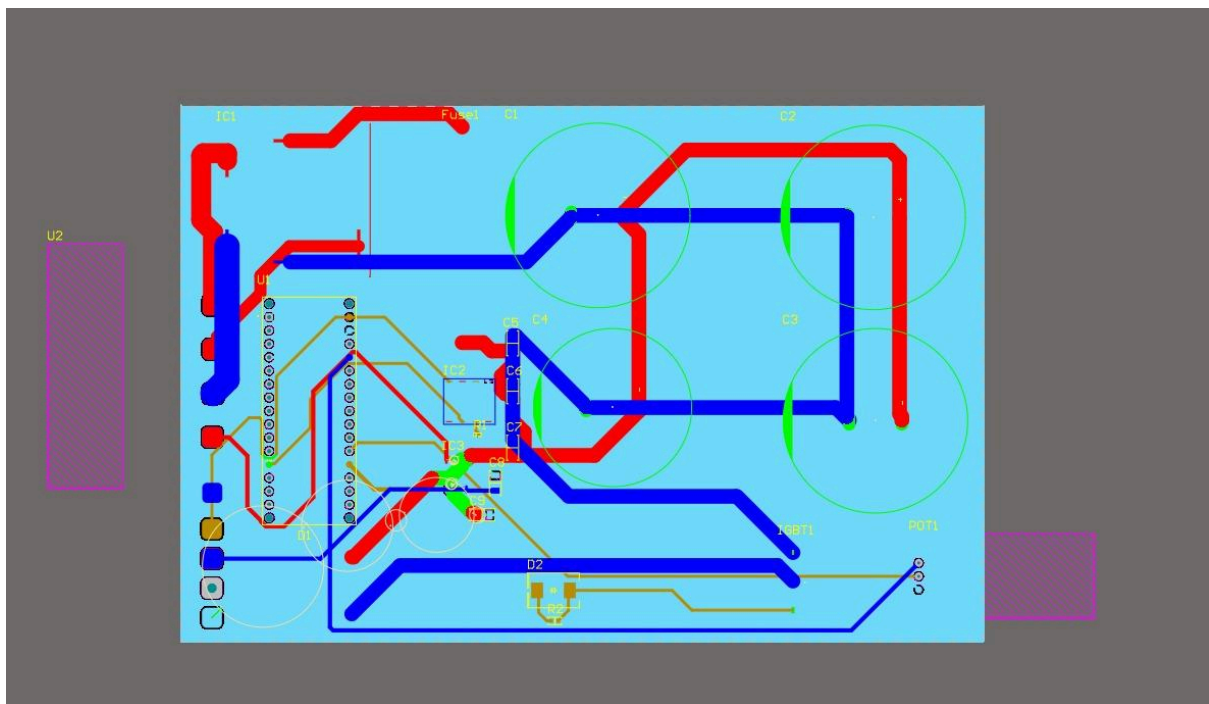


Figure 8.5: Copper Paths of Bottom Layer

Since the rectifier, IGBT, and diode are the components that generate the most heat on the board, they were positioned as far apart as possible. To cool these three components, heat sinks were added to the top of the case, designed to directly contact the components. To enable rapid cooling, these heat sinks were designed to be as thick as possible. Additionally, a heat sink was designed to cool the entire board. Each fin has a width of 1.5 mm, and the spacing between fins was set to approximately five times this width (7 mm) to ensure adequate airflow. Heat sinks were added to both the upper and lateral surfaces.

Nine holes were created for cable connections, designed to match the diameters and spacing of the cables. Care was taken to prevent interference between the currents passing through the cables. A separate hole was also created on another surface for the potentiometer. The board was designed to be inserted into the case from its bottom surface.

The PCB has a width of 102.895 mm and a length of 155.254 mm. The case was designed with a width of 109 mm, a length of 164 mm, and a height of 69 mm. The thickness of the case walls was set to 2 mm, measured from the outside to the inside. Space was allocated for thermal paste application.

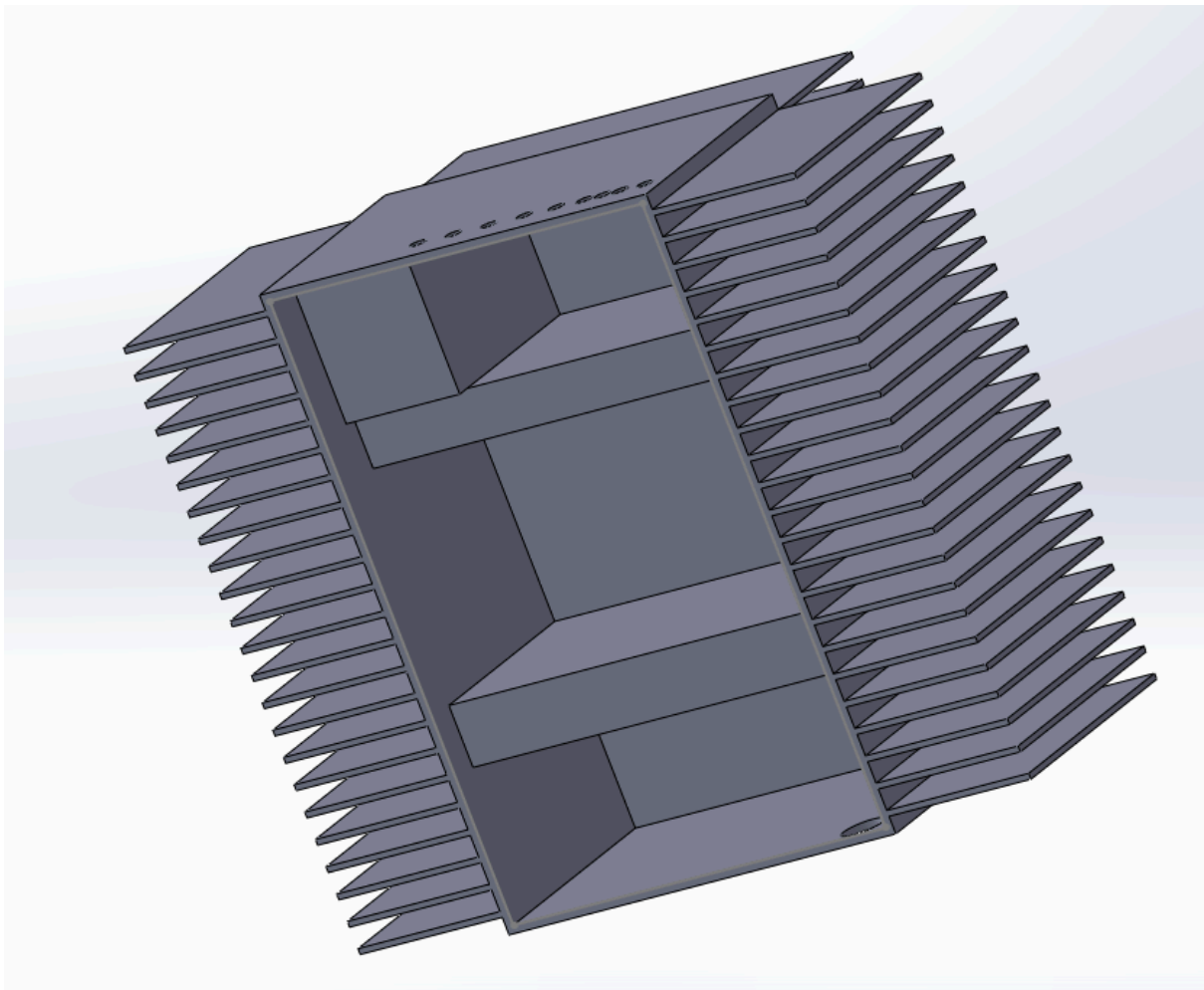


Figure 8.6: 3D view of the bottom part of the casing and heat sink

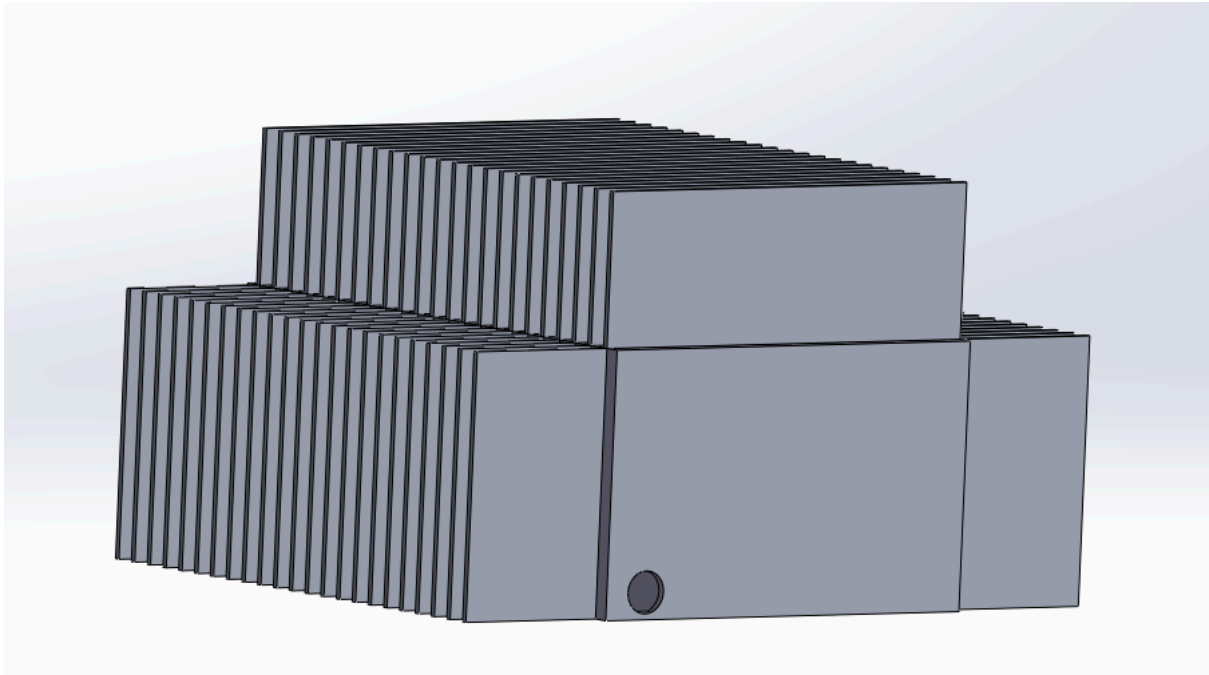


Figure 8.7: 3D view of the side part of the casing and heat sink (a)

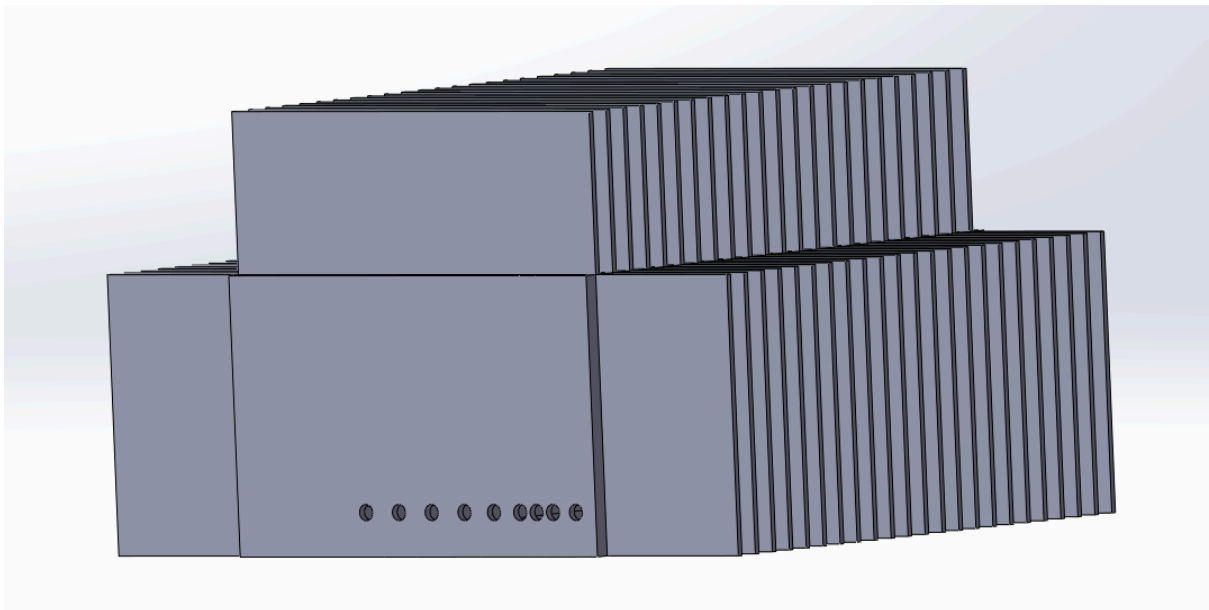


Figure 8.8: 3D view of the side part of the casing and heat sink (b)

9 - Targeted Bonuses

Thermal Simulation: We have successfully created the thermal modeling of the components such as the 3-Phase rectifier, IGBT with body diode, freewheeling diode and found suitable heatsinks for thermal dissipation.

Industrial Design: We have designed a case with proper sizing, input holes and cooling properties with 3D design of our PCB.

Tea Bonus: Our design and components are capable of supplying an output of 2 kW with the rated speed of 1500 RPM.

10 - Conclusion

The project successfully demonstrated the design and implementation of a high-performance DC motor drive system using a three-phase diode rectifier in combination with a buck converter. This topology effectively converts the three-phase AC input to a stable DC output with minimal ripple, followed by precise voltage regulation through the buck converter. The system is optimized for industrial applications, balancing simplicity, flexibility, and cost-effectiveness.

Key achievements include achieving a stable output voltage of 240 V DC with minimal ripple ($<1\%$) and the ability to operate the motor at its rated speed of 1500 RPM under a 2 kW load. The open-loop simulation validated the system's capability to supply the required voltage and torque efficiently, highlighting the reliability of the component selection and design under full-load conditions. The thermal analysis underscored the robustness of the selected components, ensuring safe and reliable operation even during worst-case scenarios. Furthermore, the PCB and casing designs incorporated effective cooling mechanisms and ensured proper component placement to minimize interference and maximize thermal dissipation.

The closed-loop control implementation further enhanced the system's performance. The PI controller successfully mitigated high inrush currents during startup, reducing peaks to safe levels, and provided precise regulation of motor speed. It demonstrated excellent tracking of the speed reference, with minimal steady-state error and robust performance under varying load conditions. The closed-loop system maintained stability and achieved reliable operation while keeping transient oscillations and thermal stress within acceptable limits.